3. EXPERIMENTAL SUMMARY

This section summarizes all of the experimental work done during this contract. Partial summaries of this work appear in the thirteen previous quarterly reports.

3.1 CONTRACT TASK 1.2. PRECIPITATED CATALYST PREPARATION METHOD DEVELOPMENT

3.1.1 INTRODUCTION

Section 3.1.2 describes the catalyst preparation method, including the pilot plant used to prepare iron/copper oxide and iron/copper/silicon oxide catalyst precursors, and the subsequent steps to furnish a properly-sized, potassium-containing oxide.

3.1.2 CATALYST PREPARATION METHOD

Catalysts were prepared by precipitation. Drawings of the precipitation plant and an enlargement of the precipitation reactor are in Figures 4 and 5 respectively. Photographs of the plant are in Figure 6. A small, but high throughput, reactor was used to mix two aqueous solutions, one containing iron and copper nitrates and the other either sodium carbonate or sodium carbonate and sodium silicate. The driving force for the precipitation was the pH change due to sodium carbonate.

In addition, water was added at two places near the bottom of the reactor to facilitate removal of precipitate.

Two pH probes were provided, one in and one below the reactor. The initial plan was to control the amount and quality of the precipitate by maintaining constant pH by frequent changes in the feed rates. Most of the precipitation runs were performed this way. Feedback control of this nature did not work because the rate of the feedback control loop was too long compared to the run length. Runs had to be short since the feed rates were very high, even though the reactor was small, resulting in a large mass of precipitate going to a very slow filtration unit. This unit consisted of a bag filter with means to collect and recycle overflow liquors. Typically about one half of the precipitate was collected on the bags during and just after the run and the remaining one half on the next day when all of the overflow liquors were filtered.

In the final mode of plant operation the feed rates were adjusted to levels known to produce near quantitative precipitation of iron, these rates were maintained during the run. Runs 30, 32 and 33 were the final runs performed during this contract and all were performed with constant feed rates. Previous runs provided material suitable for catalyst preparation even though they were not performed under conditions which allowed consistently high yields of precipitate. Figure 7 briefly outlines the conditions used for these three runs. The rate of formation of precipitate on a dry basis was 500 g/hr. Sodium silicate was only added to the sodium carbonate solution during Run 33. Plots of actual feed rates and pH's vs. time on stream for Runs 32 and 33 are in Figures 8 and 9. Throughout both runs the actual feed rates were quite steady. The reactor pH was lower and less constant than the outlet pH. The reactor pH in both runs was quite low at the beginning, perhaps

29

due to a line out problem with the pH meter. The outlet pH was about 5.5 in both Runs 32 &33.

Mass balance data for Runs 30, 32 and 33 are in Figure 10. The "direct filtered" and "overflow filtered" solids are separately reported. The total weight of iron and copper recovered increased over the three runs as the operators gained experience running the plant. Large losses can result from spills and overflows during filtration. Only small amounts of iron and copper but possibly larger amounts of silicon were lost due to solubility in the aqueous liquors. The low solubility of iron and copper are obvious from the experiment outlined in Figure 11 which reveals that 3 and 4 wt ppm, respectively, of iron and copper are soluble. These concentrations amount to losses of 0.05 wt% and 1.8 wt% of the iron and copper.

Figure 12 is the X-Ray diffraction pattern of the solid material removed as part of the experiment outlined in Figure 11. It reveals an amorphous iron oxide material, this is not surprising since the material was only dried, not calcined. As in other X-Ray spectra of materials made during this contract. the copper oxide pattern was missing. It is likely, therefore, that copper is well-dispersed throughout the iron oxide.

After sodium removal, the precipitates were further processed according to the scheme outlined in Figure 13. The final product was a material similar in size to the nominally 70 micron diameter commercial catalytic cracking catalyst. Cracking catalyst is a bound Y zeolite used for fluid catalytic cracking (not a liquid full reactor!), therefore, it is not clear whether the LPFT catalyst has to have exactly the same size. However, some lower limit on particle size will probably be needed since separation of catalyst from product wax must be done and particle size will affect the

30

ease of this separation.

Losses were taken at each step in Figure 13, those from Runs 30, 32 and 33 are summarized in Figure 14. The overall recoveries in Runs 32 and 33 were about 53% based on the amounts of iron, copper and silicon fed to the precipitation reactor. A major loss occurred during the final sizing to 140-400 mesh particles. Commercially, means would probably have to be found to recycle the through 400 mesh particles which account for the losses during sizing.

Potassium is the historic metal of choice to control activity and alpha in F-T processing. It was used in all of the catalysts of this work with the exception of one catalyst prepared during the study of the affect of the activation procedure on catalyst performance. Several ways of adding potassium were used in this work. One method used was impregnation of potassium carbonate from an aqueous solution. This is also a common method used by other F-T experimenters.

Figure 15 is a tabular summary of the on filter and overflow oxide properties from Runs 30, 32 and 33 after the work-up outlined in Figure 13. The conditions during Runs 30 and 32 were the same, and the elemental analyses of the direct and overflow filtered materials were about the same. However, there were differences in the surface area and pore volumes, the Run 32 materials having higher surface areas and lower pore volumes. Samples from Runs 30 and 32 samples were also analyzed by STEM (scanning transmission electron microscopy). Photographs resulting from these analyses are reproduced in Figures 16 and 17. The Run 32 samples contained smaller crystallites than those from Run 30. This is consistent with the higher surface area observed for these samples. Oxide samples from Runs 30 and 32 were converted to F-T catalysts and their performance in a standard slurry autoclave test were determined (Section 3.5.4, this report).

31

3.2 CONTRACT TASK 1.3. NOVEL CATALYST PREPARATION METHODS INVESTIGATION

3.2.1 INTRODUCTION

Two novel catalyst types are discussed as well as development of a method to prepare oil-dropped iron oxide spheres. One of the two catalyst types resulted from use of organo-potassium compounds to replace potassium carbonate as a source of potassium activator. The second type resulted from direct formation of high surface area potassium/iron/copper and iron/copper carbides from the corresponding oxalates followed by addition of potassium from an organo-potassium compound. Pilot plant performance data for these catalysts are in Section 3.5. The sphere forming experiments involved hydrolysis and gelation of an organo-iron compound dissolved in bubbles of mineral spirits suspended in an essentially aqueous forming liquid.

3.2.2 USE OF ORGANO-POTASSIUM COMPOUNDS

Organo-potassium compounds are soluble in organic media such as the hot oil present during LPFT. It is, therefore, possible to add such compounds to the oil and iron/copper oxide before start up or as a solution during a run. The effect of these compounds on the catalyst performance is different than expected based on work during this contract with potassium carbonate activated catalysts. Specifically, catalysts resulted which were less selective to methane + ethane. Furthermore, organo-potassium compounds are easier to employ than potassium carbonate which requires aqueous impregnation/calcination.

Three different organo-potassium compounds were used: potassium laurate, potassium benzoate and potassium nonylphenolate. Potassium laurate was the most extensively studied of the three, and produced the low selectivities mentioned above.

In some runs potassium laurate was added to the reactor with the metal oxide and start up oil before the start of a run and in other cases it was added intermittently as a solution in isopropanol/heptane during a run. Potassium laurate was also used in combination with potassium carbonate impregnation. In this case it was added as a solution to a catalyst containing potassium from potassium carbonate impregnation.

Potassium laurate-derived catalysts were less active at a given potassium level than those from potassium carbonate. However, they continued to gain activity at high potassium levels which levels resulted in activity loss when potassium carbonate was used. Methane + ethane selectivity continued to decrease at high potassium levels regardless of the potassium source.

Potassium nonylphenolate was evaluated in just one run. It was added intermittently as a solution in isopropanol/heptane to a catalyst which contained some potassium from potassium carbonate. In this case the effects on conversions and methane + ethane selectivity were directionally the same as with potassium laurate. However, the amount of change in these two was much less per gram of potassium than with potassium laurate.

Potassium benzoate was also evaluated in one run. In this run potassium laurate was added to the iron oxide at start up to furnish the initial potassium. Later an isopropanol solution of potassium benzoate was added. Addition of potassium benzoate produced a slight increase in the carbon

dioxide selectivity but no change in conversions or light ends selectivities.

The actual tests of the organo-potassium-derived catalysts are outlined in Section 3.5 along with tabular comparisons to a potassium carbonate-derived reference catalyst.

Koebel in his seminal LPFT studies used organo-potassium compounds as well as inorganic ones.[101] Claim 1 of the above referenced patent is to an improved process *"which comprises continuously passing a synthesis gas into a hydrocarbon oil product suspension of carbon monoxide hydrogenation catalyst having a concentration......................"* Clearly this is a process description of LPFT.
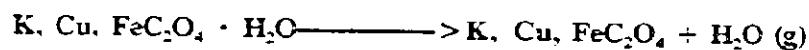
A subsidiary claim of the Koebel patent describes the alkali component of the catalyst for this process: *"Improvement according to claim 9 in which said suspension within said reactor possesses a predetermined alkali content, and in which said alkali content is maintained substantially constant by adding together with said replacing oxidic compound a catalyst based percentage of alkali material higher than that of said predetermined alkali content."* Another subsidiary claim describes use of surface tension modifying agents; potassium stearate is a specific example given in the body of the patent.

Although Koebel describes the use of potassium stearate, and makes a comment in the body that the surface tension modifying agent might be one which increases or decreases the surface tension, he does not describe a special effect on conversion and/or selectivity. The use of an organo-potassium compound to facilitate low methane + ethane selectivity at high conversion seems unique to the current work. Furthermore, it has been found that all organo-potassium compounds do not behave in the same way when added to the catalyst system in solution during a run.
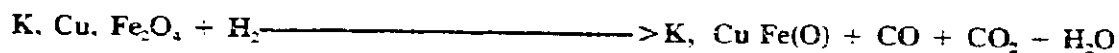
3.2.3 NOVEL METAL OXALATE-DERIVED CATALYSTS

Preparation of F-T catalysts via decomposition of metal complexes is known but has not been extensively developed[63, 102-104]. However Soong, et. al.[63] did decompose $MnFe_2(C_2O_4)_3$ to form an iron/manganese F-T catalyst. This method was used during this contract to convert a mixture of potassium, copper and iron or copper and iron oxalates into high surface area mixtures of iron carbides by the steps below:
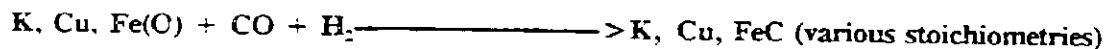
Heat, Vac

$$K, Cu, FeC_2O_4 \cdot H_2O \longrightarrow K, Cu, FeC_2O_4 + H_2O \ (g)$$

250-300° C, Atm. Pressure

$$K, Cu, Fe_2O_4 + H_2 \longrightarrow K, Cu \ Fe(0) + CO + CO_2 - H_2O$$

65 psig, 250-300° C

$$K, Cu, Fe(0) + CO + H_2 \longrightarrow K, Cu, FeC \ (various \ stoichiometries)$$

The preparation above was accomplished in a modified Mettler TA-2 thermal analytical balance. This allowed careful measurement of the mass changes as the various steps of the synthesis were performed. The oxalate decomposition step was performed with pure hydrogen. To accomplish the third step the pressure was first raised to 65 psig with hydrogen, then the carbon monoxide was added to the gas flow. The change in mass indicated that carbides were formed within less than an hour. Thereafter, F-T activity was demonstrated by the accumulation of wax in the analytical balance, as witnessed by a weight gain and actual wax accumulations in the apparatus.

Furthermore, careful analysis of the gas exiting the analytical balance showed the presence of typical F-T product gases such as methane and ethane. Several such carbide preparations were performed and the products were allowed to operate as F-T catalysts in the thermal balance for extended periods of time. It was thus found that the oxalate-derived carbides were stable at 250° C during 100-120 hour runs with either 2 : 1 or 1 : 1 molar hydrogen : carbon monoxide. However, at 300° C the catalyst lost all activity after fifty hours. An X-Ray diffraction analysis of a wax/catalyst sample was removed from the analytical balance is attached as Figure 18. This analysis indicates the presence of Fe_5C_2 and $Fe_{2.2}C$ and possibly several others as well.

A report summarizing this work more fully is attached as Appendix 3. A large sample of a copper/iron carbide was prepared in a similar fashion and evaluated in the autoclave pilot plant with potassium added as potassium laurate; its performance is outlined in Section 3.5.

3.2.4 OIL-FORMED IRON OXIDE SPHERES FROM A SOL-GEL ROUTE

The sol-gel method of preparing iron oxide catalysts is a desirable approach for improving catalyst mechanical strength because this method allows formation of spheres which are the most attrition resistant shape for catalyst particles.

The preparation of binderless iron oxide spheres has been achieved by the development of a novel sol-gel forming procedure. The starting material is a solution of Fe(III) 2-ethylhexanoate in mineral spirits which is added dropwise to an ammoniacal solution of methanol. The low viscosity of the methanol causes the formation of small droplets of the iron solution. The immiscibility of the mineral spirit solution in the methanol, and the difference in surface tensions between the two

solutions, causes the droplets to assume a spherical shape. Low levels of ammonia and water in the methanol promote the hydrolysis of the Fe(III) 2-ethylhexanoate causing the spherical particles to gel (harden). The iron containing spheres can then be isolated by filtration. These are the first reported spheres of 100% iron oxide phase, prepared without a binder. Initial preparations have resulted in 100-200μ diameter spheres.

Some as yet insurmountable mechanical difficulties were encountered in the scale-up of this new method. The principal problem results because the current method for introducing appropriate size liquid droplets of the Fe(III) 2-ethylhexanoate into the forming liquid is inadequate. This method does not control the associated formation of "powder" material, which consists of very tiny (1-10μ), but spherical particles. Several alternate methods of addition were tried. These included several sizes of eye droppers and a variety of air brush fittings. The droplets formed using the eye droppers were too large to be supported by the low viscosity methanol and broke up into smaller droplets. This left a trail of the aforementioned powder. The air brush was used in an attempt to break up the solution into a finer stream of particles before entering the methanol solution. This method reduced the number of particles having a spherical shape, presumable due to loss of too much solvent from the Fe(III) 2-ethylhexanoate solution prior to contact with the ammoniacal methanol forming solution. It might be possible to overcome this problem by increasing the dilution of the Fe(III) 2-ethylhexanoate prior to passing it through the air brush assembly.

Optimization of the level of ammonia in the methanol solution depended on the size of the Fe(III) 2-ethylhexanoate droplets. A range of 2.5—>5.0 wt% aqueous ammonium hydroxide worked best when an eye dropper was used to form the droplets. The use of higher levels of ammonia with the eye dropper, did not permit the droplets to break up. This resulted in incomplete hydrolysis

throughout the, now very large, spheres. The introduction of smaller initial droplet sizes permits the use of a higher ammonia concentration and speeds up hydrolysis. An upper limit on the aqueous ammonia addition is reached when the density of the ammoniacal methanol becomes too high, relative to that of the mineral spirit solution of Fe(III) 2-ethylhexanoate, and the droplets no longer sink through the forming medium.

3.3 CONTRACT TASK 3.3. CATALYST ACTIVATION

3.3.1 INTRODUCTION

During use the iron-based F-T catalyst is known to consist of oxidic as well as carbidic iron. In addition, several iron carbides have been characterized in the working F-T catalyst. Therefore, it might be possible to alter the performance of the catalyst by changing the types and/or amounts of the various iron species present during operation. One way to do this might be by changing the composition of the catalyst through activation procedure changes. Two activation procedures have been used in this work. In the first the catalyst was pretreated with the 0.7 molar hydrogen : carbon monoxide ratio synthesis gas which was also the plant feed. In the second the catalyst was pretreated with carbon monoxide. The catalyst performance was affected by the activation procedure.

38

3.3.2 ACTIVATION WITH SYNTHESIS GAS

The feed gas in all of this work was a simulated coal-derived synthesis gas with a H_2 : CO molar ratio of 0.7. In most of the catalyst evaluations during this contract the feed itself was used to activate the catalyst. Performance results with catalysts activated in this fashion are in Sections 3.5->3.7. In these cases the pretreatment occurred after the iron/copper oxide and start up oil were loaded into the autoclave reactor. The activation procedure was fifteen hours long during which time the feed was processed at 2.0 NL/hr · g Fe and the reactor was maintained at 280° C and 153 psig. After this the normal processing conditions of 2.4 NL/hr · g Fe, 265° C and 290 psig were established. During and after catalyst activation the stir rate was 1100 RPM. When activated in this fashion the iron/copper oxides prepared during this work produced catalysts that were moderately active and exhibited low methane + ethane selectivity. Carbon monoxide conversions with some of the better catalysts were about 70% at line out. Since the objective of this contract is a low methane + ethane catalyst, this activation procedure was used while other aspects of the catalyst which might give improved conversion and/or even lower methane + ethane selectivity were evaluated. For instance, this activation procedure was used with a series of catalysts which were similar in all regards except in the level of potassium promoter (Section 3.5.6 below). Of all the catalysts so-activated in this work, including a reference catalyst from Ruhr Chemie, the best one from the standpoint both of high conversion and low methane + ethane selectivity was the one resulting from a novel addition method of the potassium promoter. This catalyst was evaluated in Run 49 which is described in Section 3.5.7 (particularly see Figure 19). With this catalyst the carbon monoxide conversion at the standard conditions was 70% and the methane + ethane selectivity was 3.4 mole%.

3.3.3 ACTIVATION WITH CARBON MONOXIDE

Two runs were performed with catalysts resulting from carbon monoxide activation; catalyst performance results are reviewed in Section 3.5.11. In both runs the same iron/copper/silicon oxide catalyst precursor was used, the properties of which are in Figure 20. In the first run potassium was added to the catalyst composition at start up and in the second run it was added during the run. Both times the source of potassium was potassium laurate which has proven during this contract to be a way of transferring potassium to the catalyst (Section 3.5.7).

In the first run 72.7 g of iron/copper/silicon oxide along with 6.7 g of potassium laurate and 290 g of C_{30} oil were loaded into the autoclave reactor. The calculated potassium : iron weight ratio was 2.4 : 100. A carbon monoxide flow was established after the metal oxide and start up oil were added to the autoclave reactor. The activation took twenty-six hours. However, the carbon monoxide was fed to the reactor beginning at room temperature whereas in the shorter synthesis gas activations above the reactor was brought to the activation temperature under nitrogen prior to starting the synthesis gas. The reactor temperature and pressure during activation were the same as during the subsequent run, namely 265° C and 200 psig.

During activation carbon dioxide was produced by reaction of carbon monoxide with the metal oxide catalyst precursor and possibly by the Boudouard reaction as well:

$$2CO \longrightarrow C + CO_2$$
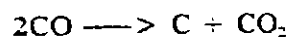
If too much carbon is formed from the Boudouard reaction, catalyst deactivation could result,

therefore, excessive activation times were avoided.

Product gas analyses during the first run's activation period are summarized in Figure 21. The amount of carbon dioxide increased as the temperature increased, but then declined shortly after the target temperature was reached, probably due to near full reduction of the iron oxide to iron carbides. A small amount of carbon dioxide was noted, however, even at the end of the activation period, possibly from the Boudouard reaction.

The second carbon monoxide activation run employed 290 g of C_{30} start up oil and a fresh 72.3 g sample of the same iron/copper/silicon oxide used in the first run. This time no potassium laurate was added at start up, but it was added as a solution in isopropanol/heptane during the run. The activation procedure was the same used in the first run; product gas analyses during the activation are summarized in Figure 22. The amount of carbon dioxide formed and the rate at which it was formed were approximately the same as in the first carbon monoxide activation run.

Independent work by Burt Davis and co-workers at the University of Kentucky as part of their current Fischer-Tropsch contract has shown that no iron oxide is left after an activation of this type. However, they find that some iron oxide is reformed during F-T synthesis. Therefore, from the standpoint of the gross structure of the operating catalyst, there do seem to be similarities regardless of the mode of activation. However, the two activation procedures do not produce catalysts which exhibit similar performance. During this work and that at the University of Kentucky more active catalysts have resulted from carbon monoxide activation than synthesis gas activation. However, carbon monoxide activation has also resulted in high methane + ethane selectivities. This selectivity resulted in part because the catalysts were so active (light ends selectivities increase at high

41

conversions). However, since the selectivity could not be effectively controlled by potassium the carbon monoxide method of catalyst activation was not pursued beyond these two runs.

3.4 CONTRACT TASK 1.5. CATALYST CHARACTERIZATION

3.4.1 INTRODUCTION

Various techniques were used to characterize fresh oxide catalyst precursors and used catalysts including scanning transmission electron microscopy (STEM). Moessbauer, X-Ray diffraction, magnetic measurements, nitrogen porosimetry and elemental analysis. Section 3.4.2 outlines experiments done with catalysts withdrawn at various times during a fifty hour run. Section 3.4.3 covers work performed to find a way to determine differences in fresh oxide mechanical strength.

3.4.2 CHARACTERIZATION OF CATALYSTS WITHDRAWN DURING FIFTY HOUR RUN

Samples of catalyst suspended in wax were withdrawn at 4, 12, 24 and 50 hours during Run 32 (a 50 hour run). These samples were analyzed by Moessbauer, X-Ray diffraction and magnetic susceptibility. The results of these tests are summarized in Figures 23-27. The Moessbauer data show the rapid conversion of Fe_2O_3 to Fe_3O_4 and a slower conversion to carbidic iron species. These changes began during the catalyst activation period and continued thereafter. These results

correlate well with the X-Ray and magnetic measurements.

The X-Ray data show, in addition, that the original Fe_2O_3 had crystallites on the order of 10 nm whereas the Fe_3O_4 had crystallites of 15-25 nm.

The magnetic susceptibility data suggests that the iron carbide is accompanied by a more complex type magnetic material which could be a mixture of iron carbides and oxides. Continued reduction in magnetism as the run progressed could be indicative of formation of more highly carbonized material.

The fifty hour run was one of four, each with a fresh sample of the same catalyst. These runs demonstrated that the slurry autoclave plant could be operated in a reproducible fashion. Performance results from these runs in Section 3.5.5 illustrate that the selectivity to light products such as methane and ethane increased during the activation period. This increase continued after the activation period but at a decreasing rate. The conversions, on the other hand, increased during activation then decreased as the runs progressed. The selectivity changes thus do not seem to be tied just to conversion. The increase in light product selectivities during the early stages of a run probably are due instead to changes in the nature of the catalyst. Although these changes are complex, it is tempting to speculate that more highly oxidized catalyst is less selective to light products. If this is the case, ways might be discovered to maintain the catalyst in a more highly oxidized state during a run wherein low light product selectivity is desired.

43

3.4.3 SILICON VS. SILICON-FREE OXIDES: MECHANICAL STRENGTH

Oxides from precipitation plant Runs 32 (no silicon) and 33 (1.25 wt% silicon) were compared with respect to mechanical strength. Aqueous slurries of the two samples each with mean particle diameter slightly less than 100 μm were subjected to sonic mixing. Particle size measurements were made by a laser light scattering method at 0, 2, 5, and 10 minutes. The results summarized in Figure 28 show that the silicon-containing oxide was mechanically stronger.

3.5 CONTRACT TASK 2.0. CATALYST TESTING

3.5.1 INTRODUCTION

Section 3.5.2 describes the method of testing the catalysts including the slurry autoclave plant used for the catalyst evaluations, and the standard catalyst activation procedure. The initial runs were performed with a reference catalyst prepared during this work, and are outlined in Section 3.5.3. These runs demonstrated the reproducibility of the slurry autoclave catalyst evaluation test; during one of them catalyst samples were withdrawn intermittently between startup and fifty hours on stream to determine changes in the catalyst properties as a function of time on stream. Analyses of these withdrawn catalyst samples are reported in Section 3.4, Catalyst Characterization. Evaluation of a reference (formerly commercial) catalyst from Ruhr Chemie is outlined in Section 3.5.4. Two identical precipitation plant runs from near the end of this work provided iron/copper oxides for the pilot plant runs outlined in Section 3.5.5. When these oxides were prepared the run to run

oxide yield was high, but there were still some changes in the physical properties of the precipitates (Section 3.1). Section 3.5.6 describes evaluation of catalysts from the same lot of oxide precipitate, but with varying levels of potassium from potassium carbonate impregnation. An alternate and less time-consuming method of potassium addition was used to prepare the catalysts outlined in Section 3.5.7. Runs with additional catalysts prepared using a similar potassium addition method are reviewed in Section 3.5.8. In Section 3.5.9 two catalysts from the same precipitation run, but differing in mesh size are evaluated. The perfor nance of the novel metal oxalate-derived catalyst is outlined in Section 3.5.10. Catalyst performance after activation with carbon monoxide is described in Section 3.5.11. Evaluation of an aliquot of the catalyst manufactured by United Catalyst Inc. and evaiuated at the LaPorte, Texas slurry bubble reactor is outlined in Section 3.5.12.

3.5.2 THE CATALYST TESTING PROCEDURE

Since pilot plant-scale slurry bubble reactors are not readily available it has been the custom to screen LPFT catalysts in slurry autcclave reactors. A diagram of the slurry autoclave plant used during this contract is in Figure 29. The reactor was contained in an insulated "hot box" maintained at 130° C. Additional heat was supplied to the reactor to achieve the operational temperature which was usually 265° C, although slightly higher temperatures were sometimes desired. Figure 30 contains a sketch of the part of the plant contained in the hot box, whereas Figure 31 contains a detailed drawing of the autoclave reactor itself. The F-T reactions are very exothermic, the liquid was, therefore, hotter than the gas this allowed the liquid level to be determined from temperature measurements up and down the thermowell shown in Figure 31.

F-T catalysts are easily deactivated by feed impurities, particularly sulfur. For this reason pure carbon monoxide : hydrogen blends were purchased from Scott Specialty Gases, Troy Michigan. Furthermore the autoclave plant contained a feed pretreatment section consisting of 1265 cc of alumina spheres maintained at 210° C and 515 cc of 13X molecular sieves maintained at room temperature. The alumina and molecular sieves were replaced by fresh material twice a year.

Means were provided to remove gas and liquid from the autoclave. In both cases removal was through cylindrical stainless steel filters (shown shaded in Figure 31). These filters were 1 1/2 in. long, by 3/8 in. outside diameter (1/4 in. inside diameter), they removed all but the finest catalyst particles. The filters plugged periodically, a positive pressure of feed usually served to unplug them, however, when this failed redundant filters were available. The redundant wax filter is shown in Figure 31. An unfiltered gas outlet was also available for emergency venting. Some catalyst fines were usually observed in withdrawn liquid (wax) from the first few periods of the run. After that, however, the wax contained very little catalyst by sight or analysis.

The F-T products were collected as both gases and liquids. Two of the traps used to collect liquids were in the hot box. (Although only two are shown each had a backup as did the traps outside of the hot box. This allowed one set of traps to be emptied while the second set was collecting products.) One hot box trap contained condensate from the continuous removal of autoclave overhead gas. The other contained the wax resulting from intermittent removal of a part of the autoclave liquid phase which was done often enough to maintain the liquid level 6.5 ± 1 inches from the bottom of the autoclave. This material usually was a solid after the trap was removed from the hot box and cooled to room temperature.

46

There was a second set of three traps outside of the hot box. The first was maintained at 0° C and the second and third at -70° C. It was found during this work that the third trap was needed to collect material that would not condense in the first two.

Two on line gas chromatographs analyzed slip streams of the hot box effluent. The first one (GC-1) performed a boiling point analysis for molecules with as many as 20 carbon atoms. The sampling valve for this chromatograph was before the first of the three traps exterior to the hot box. Unfortunately the concentrations reported by this instrument were erroneous. This was the case even after attempts to adequately heat the line and sampling valve. Heavy molecules appeared to condense into the line and/or valve during the time between samplings resulting in injection of a heavies-rich sample into the GC. The sampling valve for the second GC (GC-2) was between the first and second exterior trap. This GC performed a gas analysis and worked well. For purposes of mass balancing the plant and calculating Schulz-Flory data, this GC was used to obtain the weights of C_1-C_4 hydrocarbons. The amounts of these hydrocarbons in the first external trap were added to the GC-2 amounts, but this was a small correction. Oxygenates are not available from GC-2. in cases where selectivities to these products are reported GC-1 data were used. Most of the oxygenates were alcohols, aldehydes were found but in low levels.

The products collected in the traps were sometimes submitted for off line analyses. In cases where a Schulz-Flory plot was desired this had to be done. The sample from the hot box trap which resulted from autoclave liquid withdrawals was analyzed by liquid phase chromatography. This sample was usually a solid wax. The other hot box sample and the hydrocarbon samples in the external traps were analyzed by a boiling point gas chromatographic method. The aqueous products, which were found only in the traps external to the hot box, were analyzed for organic

47

molecules by gas chromatography. A complete breakdown of the products by carbon number was obtained by these off line analyses combined with the on line gas analysis for C_1-C_4 hydrocarbons

Conversions and selectivities were calculated with the aid of an argon internal standard in the 0.7 molar H_2 : CO feed. Selectivities reported are on a carbon dioxide-free basis. In other words, since about one half of the carbon monoxide was converted to carbon dioxide, the reported hydrocarbon selectivities are about twice what they would be if carbon dioxide selectivity were taken into account in their calculation.

In this work 72.7 g of oxide were usually used, however, in some cases 25 g were used. The high oxide amount provides 20 wt% solids in the slurry which is the target of this contract. The lower solids level was originally used for catalysts which were in short supply, however, reference runs at this loading were also performed. In all cases 290 g of a product from the Ethyl Corp. was loaded with the oxide. It is called Ethylflo 30 and is essentially a C_{30} oil. In most cases this worked well as a start up oil to be replaced during a run by product wax. The exception occurring during evaluation of catalysts which produced low levels of wax, in such cases the C_{30} oil exited with the autoclave vapors faster than it could be replaced by heavy reaction products.

High loading of catalyst into the slurry oil will be a key to the success of LPFT processing. At 72.7 g of oxide and 290 g of oil a 20 wt% loading is attained. This is now considered to be a high enough loading to be a target for this contract.

3.5.3 CERTIFICATION OF THE SLURRY AUTOCLAVE TESTING PROCEDURE

Four runs were performed with separate fresh samples of the same oxide to evaluate run to run reproducibility of the autoclave plant. Properties of this oxide are summarized in Figure 32. One of these was a short run (50 hours) from which catalyst samples were periodically withdrawn for characterization, the results of which are summarized in Section 3.4 of this report.

The activation procedure for the four reproducibility runs was the one used subsequently for most of the other runs during this work. It consisted of a fifteen hour pretreatment with the synthesis gas feed at 2.0 NL/hr·g Fe, 280° C, and 153 psig plant pressure. The stir rate before and after pretreatment was 1100 rpm. After pretreatment the operating conditions were: 2.4 NL/hr·g Fe, 265° C and 290 psig.

Performance data for the three longer runs are compared in Figures 33-39. The conversions, light product selectivities and H_2/CO usage were all closely reproduced in each run. The data for the short run were also virtually superimposable on that from the first fifty hours of the three longer runs. One reason for this was the extreme care taken to control the temperature (Figure 33).

The conversions followed a pattern observed for many iron catalysts in this work: a rapid conversion increase during the activation period followed by a line out period during which the conversions (and selectivities) were changing—in this case the conversions decreased and the light hydrocarbon selectivities increased. These changes were still taking place at the ends of the runs albeit at ever slower rates.

49

The selectivities changed due to the catalyst aging process, not due to the change in conversion. For instance, it will be shown below that the conversion/selectivity relation on a similar, but lined out, catalyst was just the opposite to that above—lower conversions in that case resulted in lower methane selectivities. Conversion changes with the lined out catalyst resulted from feed rate changes. It is possible that operating conditions can be found to maintain the low methane + ethane selective iron phase(s) present during the early part of a run. This has not been done during the current work.

3.5.4 EVALUATION OF REFERENCE RUHR CHEMIE CATALYST

Ruhr used to furnish commercial quantities of an oxidic F-T catalyst precursor. Although no longer available in large quantities, small samples are available for use as a reference. The properties of this material as measured at UOP are in Figure 40. It was evaluated in the slurry autoclave plant under the conditions used for most of the tests in this contract (Figure 41). The conversions from this catalyst were not extraordinary compared to the catalysts developed during this contract (Figure 42). The selectivities to light products were high compared to the objectives of this contract and to catalysts developed under it (Figures 43-47). For instance, at the end of the 250 hour run when the catalyst appeared to be nearly lined out the methane + ethane selectivity was 7.7 mole % (72% CO conversion).

3.5.5 COMPARISON OF CATALYSTS FROM IDENTICAL PRECIPITATION RUNS

Four catalysts were evaluated, two each from precipitation Runs 30 and 32 oxides (one direct and

one overflow filtered sample per run). In these runs 25 g of iron/copper oxide were used, with 290 g of oil. Potassium was added as solid potassium laurate along with the oxide and oil. Enough potassium laurate was used so that the iron : potassium wt. ratio was 100 : 1.8. The 0.7 molar H_2:CO feed was used. The operating conditions before and after the activation were the same as outlined in Section 3.5.2 except the feed rates were 5.8 and 7.0 NL/hr·g Fe respectively. Because of the higher feed space velocity the conversions during these runs were lower than usual. Furthermore, the percent less of conversion during line out was high (Figure 48). This was probably due to the first order nature of the conversion; a similar loss of activity can cause a greater or lesser loss in conversion depending upon whether the initial conversion was in the relatively flat or more steeply inflected part of the conversion/contact time plot.

A tabular summary of line out conversions and selectivities is in Figure 49. The catalysts from precipitation plant Run 30 were less active than the ones from Run 32. In both cases the overflow material produced a more active catalyst. Although the difference in conversion between the best and worst catalyst was high, even the Run 30 overflow catalyst exhibited the high conversion expected from work with other catalysts in this contract at the target feed rate of 2.4 NL/hr·Fe (obtained by reducing the feed rate–see Figure 48).

3.5.6 COMPARISON OF CATALYSTS FROM THE SAME OXIDE BUT WITH DIFFERENT LEVELS OF POTASSIUM

Five catalysts were evaluated, each from the same oxide but with different levels of potassium from potassium carbonate impregnation/calcination. The properties of the potassium-free oxide and the

potassium-containing oxides are in Figure 50. The catalysts were evaluated under the conditions used for plant certification (Subsection 3.5.3). As in previous runs catalyst activities and selectivities changed during activation and thereafter, but apparent line out performance was eventually attained.

Carbon monoxide conversions and methane + ethane selectivities at line out are summarized in Figure 51. A plot of carbon monoxide + hydrogen conversion vs. potassium level is in Figure 52. Catalyst activity dropped for potassium levels just above 2 g/100 g Fe. Methane + ethane selectivities dropped continuously as the potassium level increased (see also Figure 53).

Olefin to paraffin ratios at 73% conversion are summarized in Figure 46 ($C_2->C_4$). A space velocity reduction was made during the run with the low activity 2.7 g K/100 g Fe catalyst so that the conversion would be the same as with lower potassium catalysts.

Carbon dioxide selectivities were always high, even for the lower activity catalyst of Run 39 (Figure 55). Alcohol selectivities ($C_1->C_4$) are summarized in Figure 56, there was little difference as the amount of potassium changed. The sum of the alcohol selectivities varied from 2.5->3.2 mole %.

The 2.06 g K/100 g Fe catalyst (Run 37) was the best of the five from the standpoint of high activity and low methane + ethane selectivity.

Product analyses of all trap products from three Run 37 periods were performed in order to determine the complete product distributions. The heavy product present in the hot box traps was analyzed by gel phase chromatography with a correction to account for any residual (start up) C_{30}

oil. The liquids in the traps outside the hot box (aqueous and hydrocarbon) were analyzed by gas chromatography. The on line gas analyzer (GC) data were used for $C_1->C_4$ hydrocarbons. Because some C_5's sand C_6's were lost during trapping/transferring, the on line boiling point GC data were used to estimate the actual C_5 and C_6 yields. Schulz-Flory plots were constructed. The low carbon number end of these plots are in Figure 57; Figure 58 contains the full-range plots. The plots are of the so-called double-alpha type. A non linear regression method similar to that of Satterfield, was used to calculate $\alpha_1 = 0.67$ and $\alpha_2 = 0.92$ (all three plots). According to Satterfield his non-linear regression α's are within 10% of the comparable linear regression α's.

The total product analyses were also used to calculate the product distribution in each of the historic fuel ranges (Figure 59). As the catalyst approached line out less gasoline and diesel, but more heavies (C_{20-}) were produced.

3.5.7 EVALUATION OF POTASSIUM LAURATE-PROMOTED CATALYSTS

Potassium laurate is a readily available organo-potassium salt which, because of its surfactant nature, enjoys solubility in organic solvents. The original idea was that potassium laurate added at the start of the run would solubilize into the hot C_{30} oil and activate the oxide. This would eliminate two steps of the previous catalyst preparation, namely aqueous impregnation of potassium carbonate followed by calcination. The patent of Koebel suggested this might work.[13] As outlined below, it is possible to utilize potassium laurate in this fashion.

In the first run with it, 10 g of solid potassium laurate was added to 72.7 g of iron/copper oxide

(properties in Figure 60) and 290 g of C_{30} oil, the calculated Fe : K weight ratio was 100 : 3.2. The activation and post activation conditions were the same used in the autoclave plant certification runs (Section 3.5.3), the catalyst conversion performance is outlined in Figure 61. The conversion was not as high as that of the best potassium carbonate-derived catalyst, however, when the conversion was increased by reducing the feed rate a very low methane + ethane selectivity resulted (3.2 mole % at 70% CO conversion, see Figures 62 and 63). Plots of C_3 and C_4 hydrocarbon and light alcohol selectivities vs. hours on stream are in figures 64 and 65.

Schulz-Flory plots were made from three periods of this run. The results are summarized in Figures 66 to 68 as the $C_1 -> C_{13}$ part of the Schulz-Flory curves. These plots contain raw data as well as the data resulting from the non linear regression analyses. The reported values for α_1 and α_2, Xi and Phi are from the non linear regression analyses. Xi is roughly equivalent to the intersection of the two "straight lines" defined by the legs of the parabolic Schulz-Flory curve. The experimental values for C_5 and C_6 tend to be low when estimated by the on line GC analysis.

A relatively high level of potassium laurate was used in the first run due to concern that some would remain in solution and be lost during the periodic withdrawals of wax from the plant. However, this was not the case, the amount of potassium removed was very close to the amount one would predict based on the small amount of iron/copper oxide (fines) known to be present in the withdrawn wax. Figure 69 is a tabular summary of the iron and potassium levels in the product wax. Thus nearly all of the potassium laurate must have "found" the catalyst, resulting in a lower activity catalyst exactly as was the case when a similar (high) potassium level was present from impregnation/calcination of potassium carbonate.

In the following two runs a solution of potassium laurate in isopropanol/heptane (50 : 50 by weight) was added after the activation period. During these runs evidence was gathered indicating that potassium laurate promotion could lead to catalysts with lower methane + ethane selectivities. In the first of the two runs potassium laurate was added to a potassium-free catalyst, and in the second it was added to a catalyst containing a low level of potassium from potassium carbonate impregnation. The properties of the two iron/copper oxide precursors are in Figure 60.

In the first run intermittent addition of the potassium laurate solution began at 175 hours on stream (Figure 98). The result was an immediate increase in the carbon dioxide selectivity indicating an increase in the catalyst's ability to oxidize carbon monoxide to carbon dioxide. Somewhat later the Fischer-Tropsch activity of the catalyst increased as well with a concomitant reduction of the light ends selectivities (Figures 99 to 104).

The F-T activity continued to increase for potassium levels up to 2.5 g potassium/100 g iron. Thereafter, until potassium addition was terminated at 3.7 g/100 g iron there were further increases in either the carbon monoxide or hydrogen conversion. The H_2/CO usage ratio also decreased until the 2.5 g of potassium level was attained, but not thereafter. The carbon dioxide selectivity reached its maximum value at this potassium level. The changes in carbon monoxide conversion and methane, ethane and carbon dioxide selectivities as a function of potassium level are summarized in Figure 105. The immediate response of the carbon dioxide selectivity to potassium addition compared to the retarded response of carbon monoxide conversion and methane and ethane selectivities might mean that the active sites for carbon monoxide oxidation and reduction are fundamentally different, with the reduction sites requiring more than one potassium. If there is more than one F-T site the more active ones might require multiple potassium atoms. Multiple

potassium sites would accumulate more slowly than one potassium sites during the initial phase of potassium addition. If multiple potassium sites are more active for the F-T reactions, they might also be intrinsically less selective for light hydrocarbons since as the catalyst activates through addition of potassium these selectivities decrease.

The maximum conversions at the 2.5 g potassium level were less than either of the 2.1 g potassium catalysts previously described: potassium carbonate impregnated and solid potassium laurate at startup. For instance, the carbon monoxide conversion was 42% compared to about 70% for the two 2.1 g potassium catalysts.

Near the end of the run the operational temperature was increased in stages to obtain selectivities at higher conversions. Space velocity changes would probably have been a better way to achieve higher conversions since the catalyst is expected to be intrinsically more selective to light products at higher temperatures. However, the $C_1 + C_2$ selectivity at 290° C and 68% carbon monoxide conversion was only 3.4 mole%! This is a very low selectivity at this conversion even at 265° C.

In the second run the potassium laurate solution was added to a catalyst which had 1.0 g of potassium carbonate-derived potassium/100 g of iron on it at startup. This catalyst was initially more active than the one used in the previous run (Figure 106). For instance, the carbon monoxide conversion was 40% at seventy hours on stream just before potassium laurate addition began at seventy-five hours on stream. This addition was again intermittent. As in the previous run potassium laurate produced an immediate increase in the carbon dioxide selectivity (Figure 106). Activity gains were noted until the addition of enough potassium laurate to bring the total amount of potassium up to 2.0 g/100 g of iron. Further potassium laurate additions produced no activity

The second potassium laurate run was identical to the first except 6.5 g of potassium laurate was used (Fe : K wt. ratio = 100 : 2.1). A catalyst resulted which was close in activity to the 100 : 2.1 catalyst (Section 3.5.6) from potassium carbonate (Figures 70 and 71). From (90-140 hours on stream the wrong feed was used, however, after reintroduction of the right one the conversions returned to values similar to what they had been before. At 150 hours on stream the catalyst appeared to be lined out and condition changes were made to determine the affect of contact time on conversions and selectivities (Figures 72 to 75). At the end of the run the original plant operating conditions were re-established; at this time the conversions and selectivities were close to what they were at 150 hours on stream. At this time the carbon monoxide conversion was 73% and the methane + ethane selectivity was 5.2 mole %.

Samples of the wax withdrawn during the first three periods were again analyzed for iron and potassium. The amount of potassium was again about what one would expect based on the assumption that all of the potassium laurate had "found" the iron and was being removed as part of the trace amount of iron catalyst fines known to pass through the wax filter system during the early stages of a run.

Selectivity/conversion plots for methane and ethane are in Figures 76 and 77. These clearly show that a problem in achieving the target low C_1 + C_2 selectivity at high conversion is the rapid increase in this selectivity at high conversion. The H_2 to CO usage is less than 0.7 (Figure 78, the shape of this plot is typical for all iron catalysts operated at less than 280° C.[19]), but increases to approach 0.7 at high conversions. The result is that at high conversions the H_2 to CO usage increases this, in turn, can favor formation of high hydrogen products such as methane and ethane are favored.

55

Contact time/yield plots are in Figures 79 to 89. Methane is formed even at low temperatures and contact time indicating it to be a direct product of F-T processing, ethylene also seems to be a direct product. However, whereas methane does not seem to be consumed once formed, ethylene appears to be (curve bends down at higher contact times). Ethane appears to be a product of secondary synthesis (zero or near zero yield at low contact times, but rapid, non linear, yield increase at high contact times). Most logically ethane comes from hydrogenation of ethylene. Ethanol seems, at least in part, to result from direct synthesis. Propylene and butylene are direct products with some indication that they are consumed in secondary reactions. Propane and butane appear to be direct products whereas propanol and butanol appear to be products of secondary synthesis.

The effect contact time changes had on carbon monoxide and hydrogen conversion is expressed in Figure 89.

Three periods during this run were fully analyzed and Schulz-Flory plots were prepared (Figures 90 to 95). The values of α_t varied from 0.65 to 0.69. The weight fractions of the total product in each of the historic fuel ranges appear in Figure 96.

At the end of the run the carbon monoxide conversion was 70% and the $C_1 + C_2$ selectivity was 5.2 mole %. This was approximately the same as the line out performance of the Run 37 (Figure 51) potassium carbonate-derived catalyst which was 5.2 mole % $C_1 + C_2$ selectivity at 73% carbon monoxide conversion. Although the performance was not improved over the earlier catalyst, potassium laurate did offer the promise of an easier catalyst preparation and work was continued on it. A tabular summary of the performance of the Runs 37, 42 and 43 catalysts is in Figure 97.

changes. However, slight decreases in both the methane and ethane selectivities were observed when the total potassium level was increased from 2.0 to 3.0 g/100 g · Fe (Figures 108 and 109). A summary plot of the response of conversions and selectivities to increases in potassium level appears in Figure 110. During the potassium laurate additions the ethylene selectivity decreased markedly from 4% to 2% (Figure 111). At three hundred and twenty-five hours on stream a significant amount of catalyst was lost from the reactor. This happened after both slurry filters plugged and the wax level had to be controlled by removal from the non-filtered outlet. After the catalyst loss the feed rate was decreased in order to increase the conversion back to the previous level. Although not labeled on Figure 105, the feed rate before this change was the usual 2.4 NL/hr · g Fe. Just before loss of catalyst the methane + ethane selectivity was 3.4 mole % at 70% carbon monoxide conversion! This is a very low selectivity, if catalyst had not been lost space velocity changes would have been made to allow determination of methane + ethane selectivities closer to the target CO + H₂ conversion of 88%. As with the previous run, high carbon dioxide selectivity was observed at low levels of potassium, whereas the major carbon monoxide increase occurred at higher levels of potassium.

The low methane + ethane selectivity and the fact that the conversion didn't decrease at total potassium levels greater than 2 g/100 g of iron indicate that use of potassium laurate during a run caused at least a somewhat different catalyst to form than from potassium carbonate. Propane/propylene and butane/butylene selectivities are in Figures 112 and 113.

Comparisons are made of the $C_1 -> C_4$ selectivities and olefin/paraffin ratios for the four potassium laurate runs in Figure 19. The methane + ethane selectivity was reasonably consistent at about 3.3 mole % when the high potassium catalysts of Runs 42, 46 and 49 were operated to produce 70%

carbon monoxide conversion. Extraordinary means were required to achieve this conversion during Runs 42 and 46 but not during Run 49. The high activity with a high potassium catalyst in Run 49 is also unique when compared to the catalysts described in Section 3.5.6. These earlier catalysts exhibited maximum conversion at about the 2 g/ 100 g iron level.

It is possible that potassium laurate is hydrolyzed to lauric acid and potassium hydroxide in the reactor before interacting with the catalyst. If that is the case other soluble organo-potassium salts should produce catalysts similar to the ones for potassium laurate. The runs in the next subsection were done with catalysts activated with such salts.

3.5.8 EVALUATION OF ADDITIONAL ORGANO-POTASSIUM COMPOUNDS

Potassium nonylphenolate and potassium benzoate were evaluated. In Run 63 potassium nonylphenolate was added intermittently as a solution in isopropanol/heptane to 72.3 grams a catalyst which contained 1.0 g of potassium carbonate-derived potassium/100 grams of iron (Figure 114). The catalyst appeared to have approached line out before potassium nonylphenolate addition started at ninety hours on stream; at this time the carbon monoxide conversion was 35%, and the methane and ethane selectivities were, respectively, 6.0 mole % (Figure 115) and 4.5 mole % (Figure 116). The metal oxide used was a fresh sample of the same one used in the previous Run 49. This run was performed under the same conditions but a solution of potassium laurate was added intermittently beginning at seventy-five hours on stream. Prior to these additions the catalyst was converting 40% of the carbon monoxide and exhibited methane and ethane selectivities of 6.8 and 3.5 mole % respectively (Figures 105, 108, and 109), although not exactly the performance in Run 63, it is close. Part of the difference is due to the selectivities not being completely lined out.

The potassium nonylphenolate additions did not produce the immediate and dramatic affect on performance that the potassium laurate additions did during Run 49. However, the qualitative affect of potassium nonylphenolate was in the same direction, namely increased conversions and decreased selectivities to light hydrocarbons. The catalyst did not appear to have fully lined out before addition of the potassium nonylphenolate. It is possible that the slow increase in activity after the first potassium nonylphenolate addition was just a continuation of the line out process. Both additions seemed to cause small decreases in methane selectivity. The first addition seemed to reduce the ethane selectivity somewhat, the second addition did not reduce it any further.

The difference between potassium laurate and potassium nonylphenolate addition is best illustrated by the following summary data. In Run 49, at 250 hours on stream and a total potassium level of 2.4 g/100 g of iron, the carbon monoxide conversion was 70%, and the methane and ethane selectivities were, respectively, 3.1 and 1.1 mole %. In Run 63, at 170 hours on stream and a total potassium level of 2.3 g/100 g of iron, the carbon monoxide conversion was only 50%, and the methane and ethane selectivities were, respectively, 5.0 and 2.1 mole %. Clearly potassium laurate was more effective.

The potassium laurate solution was added intermittently to Run 63 beginning at 230 hours on stream. The first such addition produced an immediate effect, after it the total potassium addition was 3.0 g/100 g of iron, the carbon monoxide conversion was 70%, and the methane and ethane selectivities were, respectively, 2.7 and 1.9. This methane selectivity was about the same as in Run 49 at a potassium level of 3.0 g/100 g of iron, but the 1.9 mole % ethane selectivity was higher (Run 49 ethane selectivity = 0.7 mole %). A final potassium laurate addition was made but operational difficulties forced the run to be stopped before the full affect of it could be ascertained. This

61

addition brought the total potassium level to 3.9 g/100 g of iron, and appeared to cause additional, but smaller, decreases in the methane and ethane selectivities which were 1.9 and 1.1 at run's end. A tabular summary of Runs 49 and 63 including $C_1 - > C_4$ selectivities is in Figure 117. During Run 63 the potassium laurate additions also caused a lowering of the pro- pane/propylene and butane/butylene selectivities (Figures 118 and 119).

Potassium benzoate was added near the end of Run 65. This run employed 25 grams of "direct filtered" metal oxide from Run 32 of the oxide precipitation plant. Primarily, this run was part of the study of catalysts from identical precipitation runs outlined in Section 3.5.5. The run conditions are in this previous section, however, it should be reiterated here that solid potassium laurate was added to the reactor at start up. Catalyst performance before addition of potassium benzoate was earlier summarized in Figure 49. The autoclave runs are time-consuming to start and whenever possible attempts were made to obtain some extra knowledge after the primary run objectives were achieved. In this run one addition of potassium benzoate in isopropanol solution was made beginning at 270 hours on stream (Figure 120). Although the increase in total potassium was from 1.8 to 3.0 grams/100 grams of iron, the conversions were barely affected (Figure 121). The increases in light end selectivities (Figures 122 to 124) were due to the increased carbon dioxide selectivity; the uncorrected light ends selectivities were unchanged by the potassium benzoate addition. The increased carbon dioxide selectivity could have been due to the potassium benzoate catalyzing the Boudouard reaction to some extent.

The differences in the way the three organo-potassium compounds effect the catalyst must be related to the different types of anions present. The simplest explanation is that the benzoate and nonylphenolate solubilize the potassium to such an extent that it does not "find" the catalyst surface,

and is, in fact, eventually lost into the withdrawn product wax. However, there are other explanations such as effects of the anions on adsorbed potassium. These mechanisms can only be differentiated with additional experiments.

3.5.9 EFFECT OF CATALYST PARTICLE SIZE ON PERFORMANCE

A sample of the through 400 mesh metal oxide which resulted during sizing of the product from one of the two identical precipitation runs was compared to the sized (through 140 on 400 mesh) material. Summaries of oxide properties are in Figure 125 and performance data after line out is in Figure 126. The catalyst evaluation conditions are in Section 3.5.5.

The catalysts reached an apparent conversion line out after 125 hours on stream. At this time the carbon monoxide was about 40% from the through 400 mesh catalyst and 20% from the other one. Although selectivities from the coarse catalyst reached apparent line out at this time also, those from the through 400 mesh catalyst still were changing at the end of the 240 hour run.The finer mesh catalyst reached an apparent conversion line out after two hundred hours on stream when the carbon monoxide conversion was 39%. The through 140 on 400 mesh material reached an apparent conversion line out after 125 hours on stream when the carbon monoxide conversion was 20% (Figure 127). Of the two catalysts, the finer mesh one was more selective for light hydrocarbons. perhaps in part because the selectivities were obtained at a higher conversion.

The conversions from the two catalysts did not converge at line out as might have been expected if they were both attrited to the same mesh size by line out. The conversion difference between the two catalysts might indicate some diffusion resistance.

3.5.10 EVALUATION OF A METAL OXALATE-DERIVED CATALYST

One run was performed with a catalyst which resulted from decomposition of a mixture of iron and copper oxalates (Section 3.2.2). It was a very powdery material, its performance, therefore, was compared to that of the through 400 mesh oxide evaluated in Section 3.5.9. The physical properties and performance of these two oxides can be compared in, respectively, Figures 125 and 126. The performance data summarized in the latter Figure was after the oxalate-derived catalyst had lined out. Performance of these two materials as a function of hours on stream is in Figures 128-134. At the end of the run, the oxalate catalyst was slightly less selective for light products than the reference catalyst.

3.5.11 EVALUATION OF CARBON MONOXIDE-ACTIVATED CATALYSTS

Two runs were performed with carbon monoxide-activated catalysts. Each used a fresh 72.3 g sample of the same iron/copper/silicon oxide catalyst precursor, the properties of which are in Figure 20. In the first run the reactor was loaded with the oxide, 290 g of C_{30} oil and 6.7 g of potassium laurate (2.4 g K/100 g Fe). In the second run no potassium laurate was present at start up but a solution of it was added later. Details of the catalyst activation procedure were outlined in Section 3.3.3 and Figures 21 and 22.

Compared to synthesis gas activation, carbon monoxide activation produced a more active catalyst. For instance, in the first run the carbon monoxide conversion appeared to have lined out at 90% at the end of the ninety-six hour run (Figure 135). Plant operational problems forced early

termination of this run. At run's end the carbon monoxide + hydrogen conversion was 85% which is very close to the contract target of 88%. However, the methane and ethane selectivities were very high, although the methane selectivity had not yet lined out and was decreasing somewhat as the catalyst aged (Figures 136 and 137). The propane and propylene selectivities also had not reached line out and were also decreasing as the catalyst aged (Figure 138). The on line gas chromatograph was not separating the butane and butylene during this run, therefore, these selectivities are not available. The light alcohol selectivities were very low as they were during runs with catalysts resulting from synthesis gas activation (Figure 139).

The activation procedure for the second run was the same as the first. Potassium laurate was not added at the beginning of the run, but it was added intermittently during the run as a solution in a 50 : 50 weight blend of heptane/isopropanol. The initial conversions were about the same as in the first run, but after the addition of potassium laurate started they increased slightly the decreased (Figure 140). The performance of the two carbon monoxide activated catalysts are compared at similar times on stream and conversions in tabular fashion in Figure 141. A complete set of selectivities vs. hours on stream are in Figures 141 to 146. The potassium laurate at levels much above 1.0 g/100 g Fe appeared to cause changes in selectivities. For instance, at a cumulative potassium level of 1.5 g/100 g of iron the ethylene selectivity began to increase, however, the ethane selectivity stayed relatively constant until the potassium level reached 2.1 g/100 g of iron after which it decreased.

After the final addition of potassium laurate the conversion decreased over about one hundred and eighty hours. The nature of the catalyst was apparently changing very slowly; similar line outs were noted during the first one hundred to two hundred hours of runs wherein synthesis gas activation

was employed. At the end of the run the catalyst activity was apparently lined out and still fairly high compared to catalysts from synthesis gas activation (82% vs. 69-73% for the best synthesis gas activated catalysts). However, the methane + ethane selectivity was still unacceptably high (Figure 141).

Although carbon monoxide activation produced very active catalysts, the methane + ethane selectivities were unacceptable for the objective of this contract which requires this selectivity to be $\leq$ 5 mole %. The usual way of minimizing light hydrocarbon selectivity, namely the addition of potassium to the catalyst composition, has, so far, not caused sufficient lowering of the methane + ethane selectivity.

3.5.12 EVALUATION OF A UCI CATALYST: CROSSOVER TO SLURRY BUBBLE REACTOR

United Catalysts Inc. manufactured a large lot of metal oxide for the first slurry bubble reactor run at the LaPorte, Texas plant. A fresh aliquot from an 800 lb composite of this material was evaluated and compared to results from the run at LaPorte. The physical properties of this metal oxide are in Figure 147. The performance summary is in Figures 148 to 152 as a series of performance vs. hours on stream plots.

The catalyst activation was the standard one with synthesis gas. The initial operating conditions were 2.5 NL/Hr · g of Fe, 2.) psig and 265° C. The catalyst was quite active, for instance, the carbon monoxide conversion was stable at 80% over the first two hundred hours of operation

(Figure 148). Operational problems resulted in loss of all selectivity data from one hundred to two hundred hours on stream, however at 100 hours the methane + ethane selectivity was a low 3.7 mole%. At two hundred hours the feed rate was doubled resulting in an immediate drop in the conversions, for instance, carbon monoxide conversion fell to 41%. At two hundred and fifty hours tnee pressure was increased to 400 psig. This increased the conversion, but appeared to cause loss of catalyst activity. Directly after the pressure increase the carbon monoxide conversion was 58%, but after one hundred and fifty hours at this pressure it was 44%. At four hundred hours on stream the initial operating conditions were restored; the conversions, however, did not recoup to their values at two hundred hours on stream, for instance, the carbon monoxide conversion was only 41%. During the final one hundred hours of operation the conversion did appear to be constant. The methane + ethane selectivity was 4.5 mole % at the end of the run.